Carbon Letters (2022) 32:413–429
https://doi.org/10.1007/s42823-021-00304-8

Online ISSN 2233-4998
Print ISSN 1976-4251

REVIEW

Short review of utilization of electron-beam irradiation for preparing polyacrylonitrile-based carbon fibers and improving properties of carbon-fiber-reinforced thermoplastics

Seung Hwa Yoo[1]

Received: 14 October 2021 / Revised: 28 October 2021 / Accepted: 2 November 2021 / Published online: 15 November 2021

Abstract

Polyacrylonitrile (PAN)-based carbon fibers (CFs) and their composites, CF-reinforced plastics, have garnered significant interest as promising structural materials owing to their excellent properties and lightweight. Therefore, various processing technologies for fabricating these advanced materials using thermal energy have been intensively investigated and developed. In most cases, these thermal energy-based processes (heat treatment) are energy and time consuming due to the inefficient energy transfer from the source to materials. Meanwhile, advanced processing technologies that directly transfer energy to materials, such as radiation processing, have been developed and applied in several industrial sectors since the 1960s. Herein, general aspects of radiation processing and several key parameters for electron-beam (e-beam) processing are introduced, followed by a review of our previous studies pertaining to the preparation of low-cost CFs using specific and textile-grade PAN fibers and improvements in the mechanical and thermal properties of CF-reinforced thermoplastics afforded by e-beam irradiation. Radiation processing using e-beam irradiation is anticipated to be a promising method for fabricating advanced carbon materials and their composites.

Keywords Electron-beam irradiation · Polyacrylonitrile fiber · Carbon fiber · Carbon-fiber-reinforced thermoplastic · Tensile property · Thermal stability

1 Introduction

Carbon fiber (CF) is an advanced material that possesses high specific strength and high chemical and corrosion resistance compared with steel, rendering it a promising structural material [1]. CFs are typically synthesized by heating polymers, such as polyacrylonitrile (PAN) fibers, to gradually transform them to carbon with a graphitic structure. PAN fibers are heat treated by passing them through a series of ovens under gradual temperature increments and different atmospheres. Because this process is both energy and time consuming, the price of CFs is high. Therefore, to reduce the price of CFs, extensive investigations have been performed to reduce the heat treatment duration or enable the use of low-cost precursor fibers [2–5].

CFs are widely used as reinforcements for composite materials embedded in a matrix, such as polymers [6, 7]. Carbon-fiber-reinforced plastics (CFRPs) possess high strength owing to CFs, and the matrix of CRFPs effectively transfers load to the CFs. Thermoset resins are initially developed as matrices that exhibit desirable interfacial properties with CFs [8, 9]. Recently, thermoplastic resin-based CFRPs and CF-reinforced thermoplastics (CFRTPs) have been actively investigated to overcome the productivity and recycling limitations of thermoset-based CFRPs [10]. However, a few challenges associated with the intrinsic properties of thermoplastics must be addressed.

Meanwhile, the application of radiation to process materials has been developed since the 1960s [11–13]. Conventionally, polymers are irradiated with γ-rays or electron beams (e-beams) to cross-link the claddings of cable/wire, plastic foam, hydrogels, and radial tires [14]. Furthermore, thermoset resins were cured via irradiation. High-energy radiation with sufficient penetration ability

---

✉ Seung Hwa Yoo
seunghwayoo@jbnu.ac.kr

[1] Department of Quantum System Engineering, Jeonbuk National University, Jeollabuk-do, Jeonju-si, Republic of Korea

was performed to treat the bulk of the material. The main advantage of radiation processing technology is its energy efficiency: high-energy particles transfer energy directly when they penetrate the material, which enables various reactions to occur at room temperature [15, 16]. Typically, these reactions can be induced without using agents, thereby allowing the final product to be pure, without any risk associated with residual unreacted agents in the material; it is noteworthy that impurities will deteriorate the properties of the final product. Modern industrial irradiators are equipped with a conveyer system, e.g., a system that enables continuous processing to increase the productivity for mass production. Furthermore, considering technical and security aspects, e-beam irradiation is more advantageous compared with γ-ray irradiation.

This short review introduces the general aspects of radiation processing, with emphasis on e-beam irradiation, the key parameters of e-beam irradiation, and our recent study, in which e-beam irradiation was applied to fabricate low-cost CFs and improve the mechanical and thermal properties of CFRTPs.

2 Radiation processing technology

Radiation processing technology is used to treat materials (conventionally, via cross-linking/grafting/curing) in an energy- and cost-efficient manner [17, 18]. It is widely applied in several industries, such as automobile, aerospace, construction, and healthcare. The radiation type typically used in this technology is ionizing radiation, such as high-energy electrons and photons [19, 20]. The characteristics, advantages, and disadvantages of each type of radiation are summarized in Table 1.

Table 1 Comparison between ionizing radiation types frequently used in radiation processing technology

	Electron (e^-)	Photon (γ- or X-ray)
Source	Accelerators	Radioisotopes or accelerators
Charge of particle	Negative	Neutral
Interaction with matter	Directly (Coulomb force)	Indirectly
Penetration in material	Low	High
Energy absorption in material (absorbed dose rate)	High	Low
Irradiation duration	Short	Long

2.1 Electron

The high-energy e-beam used for radiation processing is generated using an electron accelerator. Accelerated electrons are irradiated to the object and then transferred by a conveyer system. To uniformly irradiate large objects, the e-beam is typically scanned using a scan magnet and spread through the scan horn equipped with an extraction window, which resembles a curtain of an electron shower spanning the conveyer width (Fig. 1). During irradiation, high-energy electrons enter the object, transfer a small portion of their energy (absorbed by the object) on penetrating the object, and finally exit the object with a reduced energy compared with the initial energy. The object is repeatedly irradiated to attain the required absorbed dose (energy absorbed per unit mass of material) by increasing the number of passes in the irradiation area. Higher initial electron energies allow a higher level of penetration through materials; however, the linear energy transfer (energy transferred to the material per unit length of radiation penetration) is lower. Therefore, the higher penetration of radiation results in lower energy transfer to the material (hence, a lower absorbed dose rate). To treat the surface of materials, low-energy (a few tens to a few hundreds of kiloelectron volts) e-beams are preferred, whereas to treat the bulk of thick materials, higher energies (a few megaelectron volts) are preferred. In regard to high-density materials, the penetration of e-beams might be limited because the penetration depth is inversely proportional to the material density. Furthermore, the absorbed dose rate of the e-beam (units: kGy/s) is much higher than that of photons (units: kGy/h); therefore, e-beams require a much shorter irradiation duration to achieve the same absorbed dose.

2.2 Photon (γ- and X-rays)

Typically, high-energy photons (γ-rays) for irradiation are generated from the spontaneous decay of radioisotopes, such as Co-60 and Cs-137. Co-60 is widely used in radiation processing. It emits two γ-rays (1.17 and 1.33 MeV) per decay, and it is often approximated as two 1.25 MeV γ-rays emitted per decay for convenience. The most prominent advantage of γ-rays is their high penetration through materials, which enables high-density materials to be treated. However, the low-energy transfer to the material (therefore, a low absorbed dose rate) requires prolonged irradiation to achieve the desirable absorbed dose, and the strengthening of regulations associated with the usage of artificial radioisotopes (e.g., Co-60 and Cs-137) promoted the utilization of e-beams. As an alternative photon source,

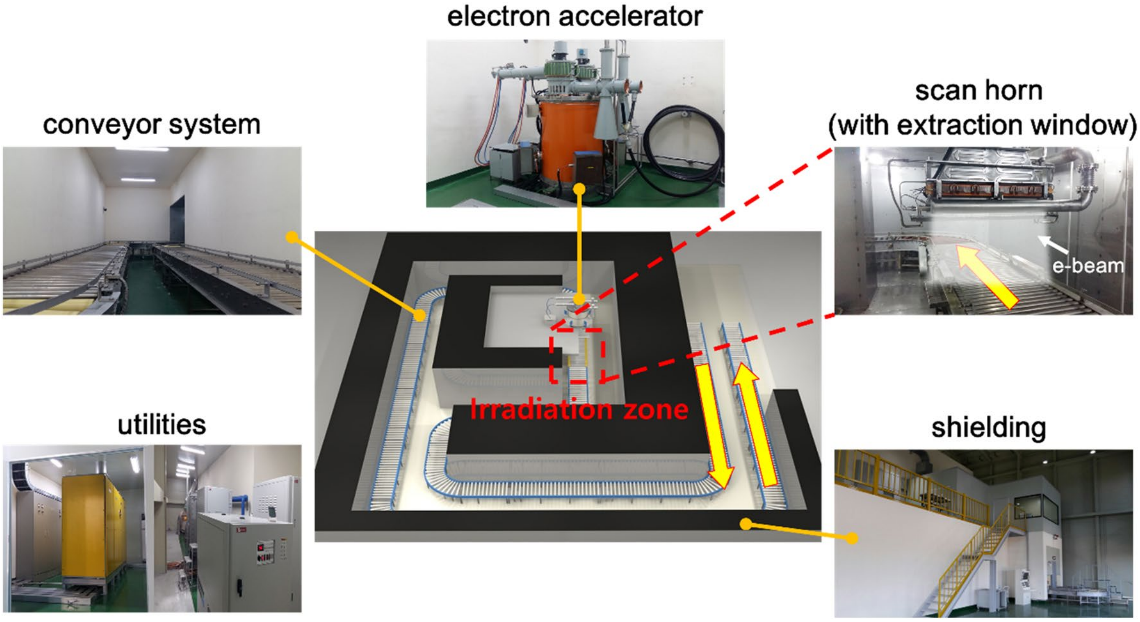

Fig. 1 Illustration of typical e-beam irradiation facility. The yellow arrow indicates the entrance and exit of the irradiated object on the conveyor. The object enters the irradiation zone, passes under the extraction window to be irradiated, and finally exits the irradiation zone

high-energy X-rays for irradiation have been adopted more frequently owing to the development of high-power electron accelerators. High-energy X-rays are generated by converting high-energy electrons to bremsstrahlung X-rays. The development of electron accelerators with high beam currents has enabled high-intensity X-rays for irradiation, which can provide sufficiently high absorbed dose rates. The irradiation process using photons is similar to that using an e-beam, in which objects are exposed to γ- or X-rays until the required absorbed dose by increasing the irradiation duration.

2.3 Key parameters for e-beam irradiation

2.3.1 Energy and current

The energy of the electrons determines the penetration depth of the object subjected to irradiation. A typical depth–dose profile of e-beam irradiation is shown in Fig. 2. The absorbed dose of the material increases gradually below the surface, maximizes at a certain depth, and decreases further. The gradual increase in absorbed dose below the surface and the further decrease after the maximum dose is attained are due to backscattered electrons generated from the interaction between the e-beam and material (the electrons of the atom), as well as the limited penetration of the e-beam, which loses energy as it penetrates through the material. For higher e-beam energies, the penetration depth and depth position at the maximum dose are higher. Therefore, low-energy (a few tens to a few hundreds of keV) is preferred for treating the surface, whereas a high energy (few MeV) is preferred for treating the bulk of thick materials, as mentioned above.

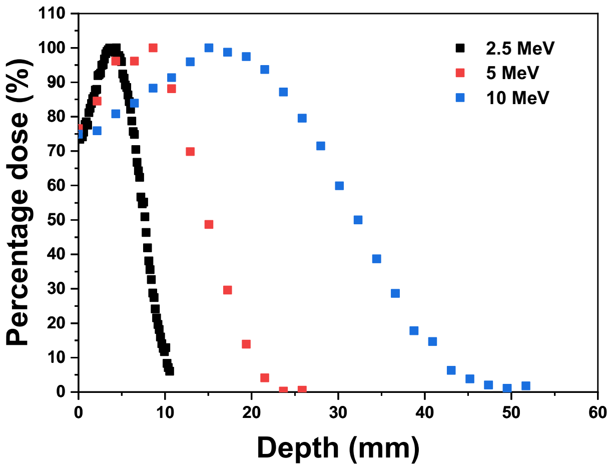

Fig. 2 Depth–dose distribution for different e-beam energies (material density: 1 g/cm^3). Percentage dose refers to dose normalized to maximum dose at fixed e-beam energy

The e-beam current indicates the number of electrons irradiating the object per unit time. A 1 mA of beam current corresponds to 6.25×10^{15} electrons traveling per second in the beam. Therefore, numerous electrons enter the material, and this phenomenon is referred to as an electron shower. The amount and rate of irradiation (as explained in Sect. 2.3.3) can be controlled by changing the beam current. Typical industrial irradiators operate at a beam current of a few to several hundreds of milliamperes, and the maximum beam current is typically higher for a lower beam energy of the electron accelerator.

2.3.2 Conveyor speed

The object (or samples) can be irradiated via one of two methods: the stationary or conveying method. In the former, samples are fixed on a stationary stage (which might be water cooled) under the extraction window, and the amount of irradiation (typically the absorbed dose) is varied by controlling the irradiation duration. However, most industrial irradiators are equipped with a conveyor system, where samples are loaded onto trays, and these trays are transferred to the irradiation zone by operating the conveyor. The sample-loaded trays are passed under the extraction window at a designated speed, and the amount of irradiation is varied by controlling the conveyor speed and accumulated number of passes under the extraction window. The conveyor speed under the extraction window is typically set to 1–15 m/min.

2.3.3 Absorbed dose and dose rate

The amount of irradiation required for radiation processing is typically quantified by estimating the absorbed dose of the sample. The absorbed dose is defined as the "energy absorbed in matter per unit mass," for which the units "Gy (J/kg)" are widely used [21]. The absorbed dose of irradiated samples can be measured using a dosimeter or evaluated via simulation-based calculations. At a specified e-beam energy, the desired absorbed dose for the samples can be obtained by controlling the beam current, conveyor speed, and number of passes. In general, the absorbed dose is directly proportional to the beam current and number of passes. By contrast, it is inversely proportional to the conveyor speed, as shown in Fig. 3.

2.3.4 Atmosphere and temperature

For general industrial irradiators, e-beam irradiation is conducted in an air atmosphere. This allows the irradiated samples to be in contact with oxygen in the air during and after irradiation. Therefore, the irradiated samples can be further oxidized by the reactive radical species formed, which subsequently react with oxygen. To prevent oxidation, the samples should be contained in a sealed container in an inert atmosphere or vacuum during and after irradiation. Oxidation might be beneficial or detrimental depending on the purpose of irradiation and the application of the irradiated material.

Most irradiation processes are performed at room temperature, whereas some are performed under cryogenic or elevated temperatures for specific purposes. Irradiation inevitably increases the temperature of the material because a portion of the absorbed dose dissipates as heat. The temperature increase by irradiation depends on the specific heat of the material and the absorbed dose/dose rate (which are inversely and approximately proportional to the specific heat and absorbed dose/dose rate, respectively). The temperature increase in the material can be suppressed by cooling the sample during irradiation or by decreasing the absorbed dose/dose rate.

3 Irradiation for preparation of PAN-based CFs

3.1 Special PAN fiber-based CF

More than 90% of commercially available CFs are PAN-based CFs synthesized using special PAN fibers as precursors. Structural changes in PAN fibers during typical stabilization and carbonization processes have been widely investigated [22–24]. The report by Hirt et al. showed that radicals such as alkyl and its peroxide were formed via the irradiation of PAN [25]. Thereafter, changes in various

Fig. 3 Relationship between absorbed dose and each of **a** beam current and **b** conveyor speed (based on 5 MeV energy and one pass under e-beam irradiation)

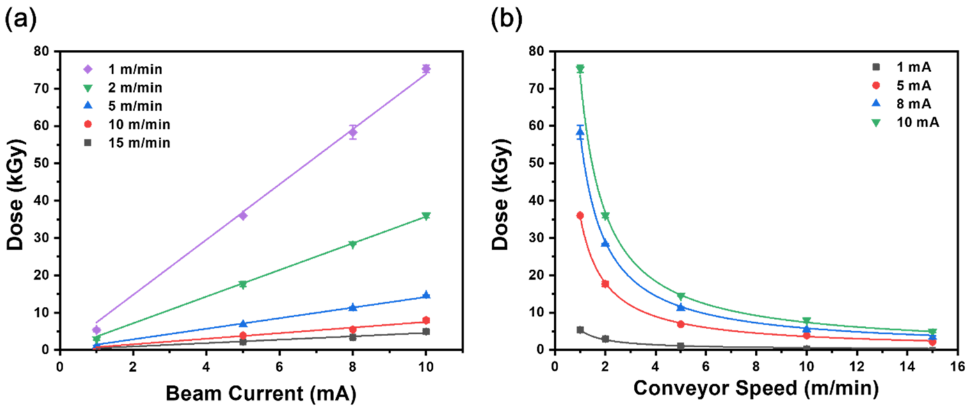

properties (physical, thermal, mechanical, and chemical properties) of PAN caused by irradiation have been extensively investigated [26], as summarized in Table 2.

The results of these studies show that various radicals were formed by irradiation, and that they mitigated the exothermal reaction of the subsequent heat treatment (stabilization process). In the typical CF production process, the exothermal reaction during stabilization should be carefully controlled to prevent the fibers from burning out. Therefore, the mitigation of this exothermal reaction using irradiated PAN fibers for the stabilization process offers significant benefits. This can be verified by performing a differential scanning calorimetry (DSC) analysis on the irradiated PAN fibers (Fig. 4). By increasing the absorbed dose, the onset temperature of the exothermal peak decreased, and peak broadening became prominent. Therefore, heat release during stabilization can be initiated at a lower temperature and proceeded in a wider temperature range, thereby rendering it easier to prevent abrupt temperature increases in the fibers during stabilization.

Another benefit of irradiating the special PAN fibers is that the duration of thermal stabilization is reduced. Various studies have shown that irradiation can generate free radicals in PAN, which can cause cross-linking and cyclization reactions (Table 2). These reactions are necessary to convert the PAN polymer into a ladder structure suitable for subsequent thermal treatment (carbonization). In our study, various radicals formed by the e-beam irradiation of special PAN fibers (Sinosteel Jilin Carbon Co., Ltd.) were analyzed via ESR spectroscopy (Fig. 5). These radicals (alkyl, allyl, and polyenyl) gradually transformed into peroxy radicals upon heating in air and promoted cyclization during thermal stabilization. Consequently, the total duration required for stabilization was reduced to one-fourth that of the conventional process by irradiating the PAN fibers prior to thermal stabilization [40].

Several research groups have attempted to fabricate CFs based on irradiated special PAN fibers and subsequent heat treatment (stabilization and carbonization), as summarized in Table 3. The most typical approach is the irradiation (primarily e-beams and γ-rays) of PAN fibers as a pretreatment, where stabilization is conducted on the irradiated PAN fibers, followed by carbonization to yield CFs [41]. In our study, CFs were fabricated by carbonizing the irradiated PAN fibers after stabilization at 1200 °C in a nitrogen atmosphere. The mechanical properties of CFs fabricated from irradiated PAN fibers were comparable to those from the conventional approach, considering that the entire process was batch-wise conducted in a laboratory. Our results indicated that 200 kGy was sufficient to fabricate CFs with a TS, a YM, and an elongation of 2.3 GPa, 216 GPa, and 1.2%, respectively (Fig. 6).

3.2 Textile-grade PAN-fiber-based CF

Several studies pertaining to the fabrication of low-cost CFs using textile-grade PAN fibers as precursors were conducted [47, 48]. Owing to the exothermic reactions of PAN fibers during thermal stabilization, the temperature of the PAN fibers increases inevitably. In textile-grade PAN fibers, high contents of co-monomers lower the melting point of PAN, and the absence of co-monomers such as itaconic acid limits the exothermic reactions in a narrow temperature range. Consequently, the heat generated by the intense exothermic reaction melts the surface of the PAN fiber and induces superficial fusion between filaments, as shown in Fig. 7a and c. Therefore, difficulty in achieving precise temperature control when fabricating CFs using textile-grade PAN fibers has hindered further relevant investigations. In this study, we attempted many combinations of heating programs based on commercial textile-grade PAN fibers provided by Taekwang Industry Co., Ltd. (Ulsan, Republic of Korea); nonetheless, we failed to fabricate CFs without superficial fusion between filaments.

To avoid superficial fusion between filaments, e-beam irradiation was applied to fabricate monofilament CFs using textile-grade PAN fibers (Figs. 7b, d, and 8). Compared with our previous study based on special PAN fibers, the textile-grade PAN fibers used in this study required a higher absorbed dose (1000 or 1500 kGy) to fabricate CFs with sufficient mechanical properties. It was demonstrated that the cross-linking and cyclization of PAN molecules initiated at lower temperatures prevented superficial fusion by suppressing surface melting, as verified via DSC and dynamic mechanical analysis (DMA) (Fig. 9). Furthermore, the mitigation of the exothermal reaction and shortening of the stabilization duration were observed.

CFs were fabricated by carbonizing irradiated textile-grade PAN fibers after thermal stabilization. To improve the mechanical properties, the textile-grade PAN fibers were hot stretched. Finally, the maximum TS, YM, and STF of the fabricated CFs were measured to be 1.83 ± 0.23 GPa, 147.44 ± 4.55 GPa, and 1.30 ± 0.15%, respectively (Fig. 10). Based on our results, we believe that e-beam irradiation is an efficient technique for fabricating CFs in an energy- and cost-efficient manner, regardless of the grade of the precursor PAN fiber. Our study was conducted in a batch-wise manner; therefore, the mechanical properties of CFs fabricated from irradiated PAN fibers can be further improved by fabricating them continuously. In fact, several recent studies have demonstrated the continuous fabrication of CFs using e-beam irradiation and heat treatment [43].

Table 2 Studies that investigated the irradiation effect on various properties and subsequent thermal stabilization of PAN fiber

PAN fiber	Irradiation				Heat treatment	Property	Ref.
	Type	Energy (MeV)/current (mA)	Absorbed dose (kGy)	Absorbed dose rate	Stabilization (°C)		
Homopolymer	Electron	1.7/32	100, 200	–	180, 200, 220, 240, 260, 280, 300	Chemical structure, transverse section, surface morphology, and thermal properties	[27]
Homopolymer		Maximum 0.18/100	100, 200, 300, 400	–	Up to 320	ESR, tensile properties	[25]
Copolymer (Blue Star Co.: 96% acrylonitrile, 3% methyl acrylate, and 1% itaconic acid)		1.14/7.6	100, 300, 500	6.67 kGy/s	240	Morphology, thermal behaviors, and molecular structure	[28]
Copolymer (Anshan East Asia Carbon Fiber Co., Ltd.)		1.14/4	500, 1000, 2000, 3000, 5000	–	–	Chemical structure, thermal, and tensile properties	[29]
Copolymer (Anshan East Asia Carbon Fiber Co., Ltd.)		1.14/4	500, 1000, 2000	–	–	Gel fraction, molecular structure, crystal structure	[30]
Copolymer (Jilin Chemical Fiber Group Co.)		0.5/10–100	50, 100, 200, 400	50–400 kGy/pass	200–260	ESR, molecular structure, thermal behavior, density	[31]
Copolymer (Jilin Chemical Fiber Group Co.)		0.5/10–100	50, 100, 200, 300, 400	2, 4, 8, 10, 13 kGy/s	60–260	ESR, thermal behavior, and surface properties	[32]
Nitron complex technical fibers (All-Russian Scientific-Research Institute of Synthetic fibers (Tver'))	γ-ray	~1.25 (Co-60)	10–2000	1–15 Gy/s	–	Thermal, mechanical, and thermo-mechanical properties, crystal structure, density	[33]
Copolymer (poly(acrylonitrile-co-methyl acrylate)			50, 100, 200, 300, 400	8.0 kGy/h	170, 190, 210, 230, 250	Molecular structure, thermal properties, ESR	[34]
Wet-spun PAN fiber containing 1.1% (mol/mol) methylacrylate			50, 100, 200, 300, 500	4.3 kGy/h	220, 250	Gel fraction, crystal structure, tensile strength, thermal properties, density	[35]
Copolymer (acrylonitrile:itaconic acid = 98.7:1.3)			50, 100	2.0 kGy/h	–	Molecular structure, thermal and thermo-mechanical properties, crystal structure	[36]
Acrylonitrile/acrylamide copolymer			50, 100, 200, 300, 400	–	270	chemical structures and thermal properties, solubility, crystal structure, thermo-mechanical properties	[37]
Wet-spun PAN fiber containing 1.1% (mol/mol) methylacrylate			50, 100, 200, 500	4.3 kGy/h	–	Gel fraction, mass change	[38]
Copolymer (Jilin Chemical Fiber)			400, 600, 800	–	–	Molecular structure, crystal structure, thermal properties, ESR, tensile strength	[39]

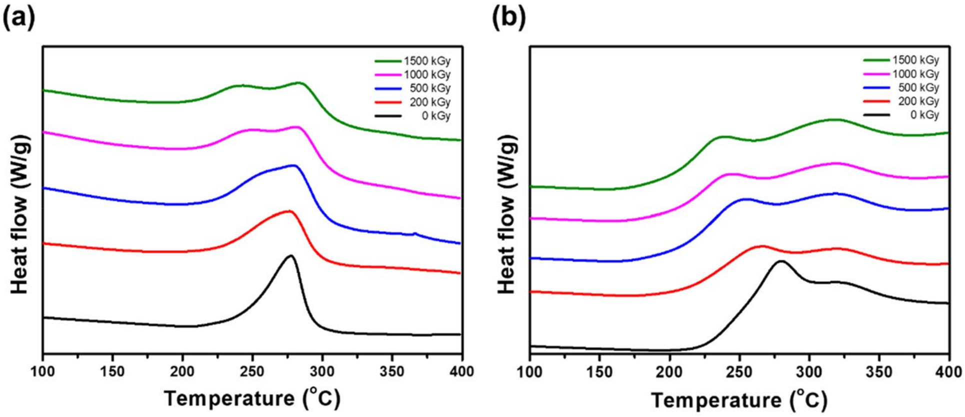

Fig. 4 DSC curves of irradiated PAN fibers measured under **a** nitrogen and **b** air atmosphere. Reprinted from [40], Copyright 2016, with permission from Springer Nature

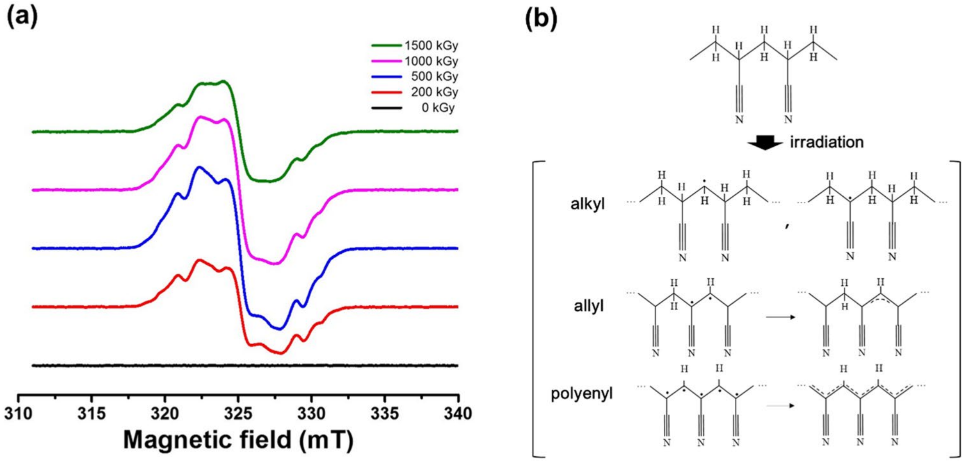

Fig. 5 **a** ESR spectra of PAN fibers irradiated for different absorbed doses. Reprinted from [40], Copyright 2016, with permission from Springer Nature. **b** Alkyl, allyl, and polyenyl radicals of irradiated PAN fibers

4 Irradiation for preparation of CFRTPs

4.1 Thermoset-matrix-based CFRPs

In the early development stages of CFRPs, thermoset resin was predominantly used as a matrix material (Fig. 11) [8, 49]. The advantages of thermoset-based CFRPs compared with conventional structural materials such as steel are their high specific strength, specific modulus, and chemical and thermal resistances; however, their applications are limited owing to their high cost, low productivity, difficulty in recycling, and weakness toward impact. Irradiation for curing thermoset resins of CFRPs have been conducted by several studies (Fig. 12a) [50–53]. Meanwhile, the surface of CFs was treated via irradiation to improve the interfacial properties of CF and resin [54–56]. In these studies, various functional groups were formed on the surface of CFs, which improved the adhesion of the CFs to the matrix resin.

4.2 CFRTPs

Recently, CFRTPs have been developed to overcome the above-mentioned disadvantages of thermoset-based CFRPs. Well-established thermoplastic processing technologies can be adopted for CFRTPs and are expected to enhance their productivity and recyclability [57–59]. However, a few challenges must be solved: the mechanical properties (except impact strength) of CFRTPs are low because of the inferior interfacial adhesion between CFs and the thermoplastic matrix. Furthermore, the intrinsic characteristics of thermoplastics limit the application of CFRTPs at high temperatures.

To address the above-mentioned issues, e-beam irradiation was applied to CFRTPs. Nishi et al. extensively investigated the effect of using homogeneous low-voltage electron-beam irradiation on various CFRTPs [60–65]. Low-energy (0.1 MeV) e-beam irradiation was conducted by repetitively

Table 3 Studies in which CFs were fabricated based on irradiated PAN fiber and subsequent heat treatment

Precursor	Irradiation				Heat treatment		Process	Mechanical properties of CF			Ref.
	Type	Energy (MeV)/current (mA)	Absorbed dose (kGy)	Absorbed dose rate	Stabilization (°C)	Carbonization (°C)		TS (GPa)	YM (GPa)	STF (%)	
Special PAN	Electron	1.5/35	1200	40^a kGy/s	190–215, 205–240, 220–255, 240–275	Low temp.: 400–700 High temp.: 1250–1350	Continuous	~1.7–2.27	~135–174	–	[42]
		1.14/8	1000	–	200 250	1200	–	0.6–2.3	–	–	[8]
		1.5/35	800	40^b kGy/s	210–225, 245–263	Low temp.: 400–700 High temp.: 1250–1350	Continuous	2.85	203	1.40	[43]
		1/1	200, 500, 1000, 1500	1 kGy/s	230	1200	Batch	2.3	216	1.2	[40]
	γ-ray	~1.25 (Co-60)	50, 100, 200, 300, 400	8.0 kGy/h	175–190, 210–220, 230–235, 240–250, 263–270	400–450–600–850–1300	Continuous	3.47	265	–	[44]
			100, 400	–	190–210, 220–230, 240–245, 250–260, 263–270	400–450–600–800–1200	Continuous	~3.5–4.25	~210–230	–	[45]
Textile-grade PAN	Electron	1/1	200, 500, 1000, 1500	1 kGy/s	100–200, 200–215, 215–230, 230–255	1200	Batch	1.46	141.35	1.07	[46]

[a] Calculated based on irradiation time of 40 s

[b] Calculated based on irradiation time of 20 s

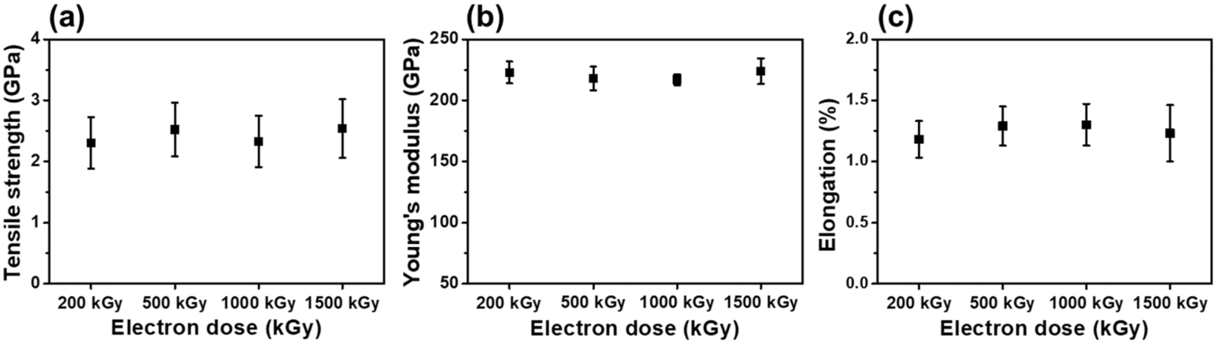

Fig. 6 TS, YM, and elongation of CFs fabricated from irradiated PAN fibers. Absorbed dose varied as 200, 500, 100, and 1500 kGy. Thermal stabilization and carbonization conducted at 230 °C for 30 min and 1200 °C, respectively. Reprinted from [40], Copyright 2016, with permission from Springer Nature

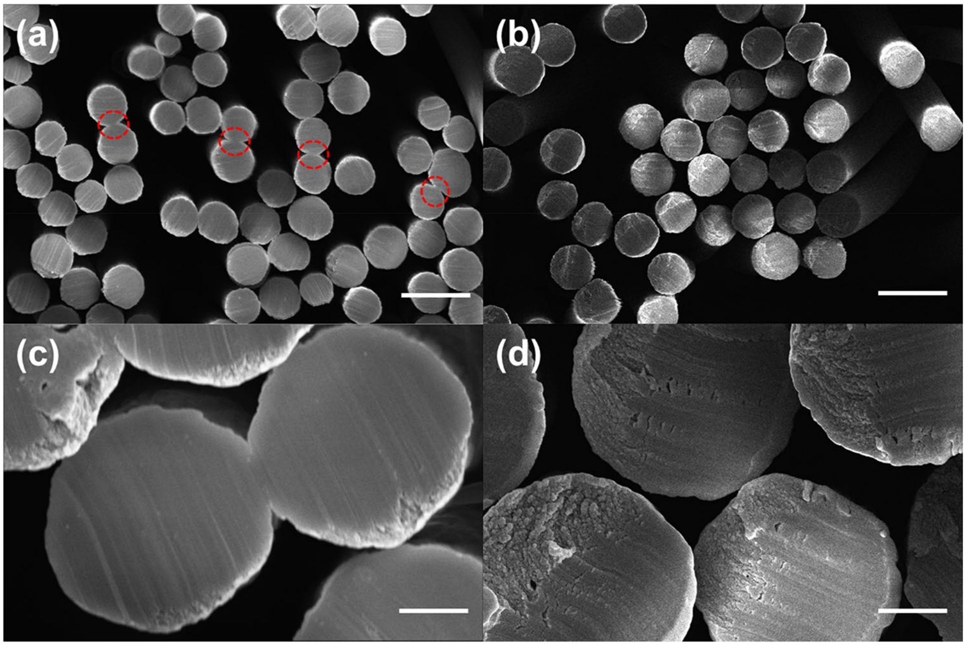

Fig. 7 SEM images of textile-grade PAN fibers heated at 200 °C for 1 h **a** without e-beam irradiation and **b** after e-beam irradiation at 1500 kGy. Dotted red circles show regions where superficial fusion occurred between filaments under condition (**a**). Scale bar corresponds to **a**, **b** 25 µm and **c**, **d** 5 µm. Reprinted from [46], Copyright 2017, with permission from Elsevier

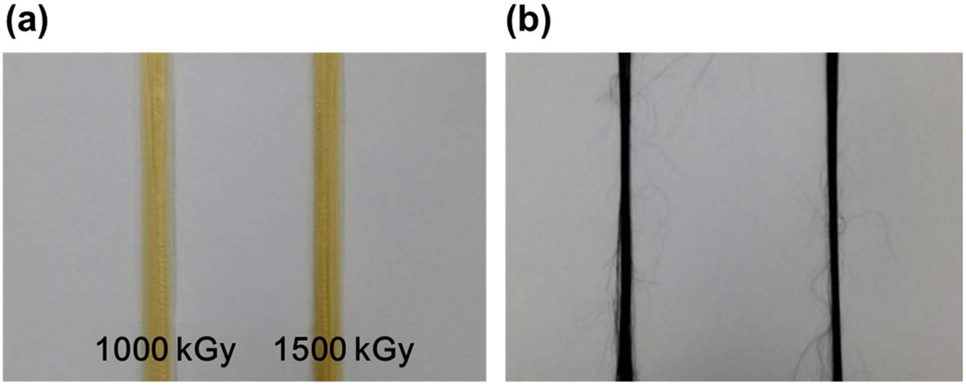

Fig. 8 Photograph of textile-grade PAN fibers after **a** irradiation and **b** thermal stabilization

conveying the samples under the irradiation zone in a nitrogen atmosphere. They explained that irradiation-induced surface activation via charging and compressive stresses at the interface via dangling bond formation in the polymer. Hence, the enhanced mechanical properties of the irradiated CFRTPs originated from the frictional force between the CF

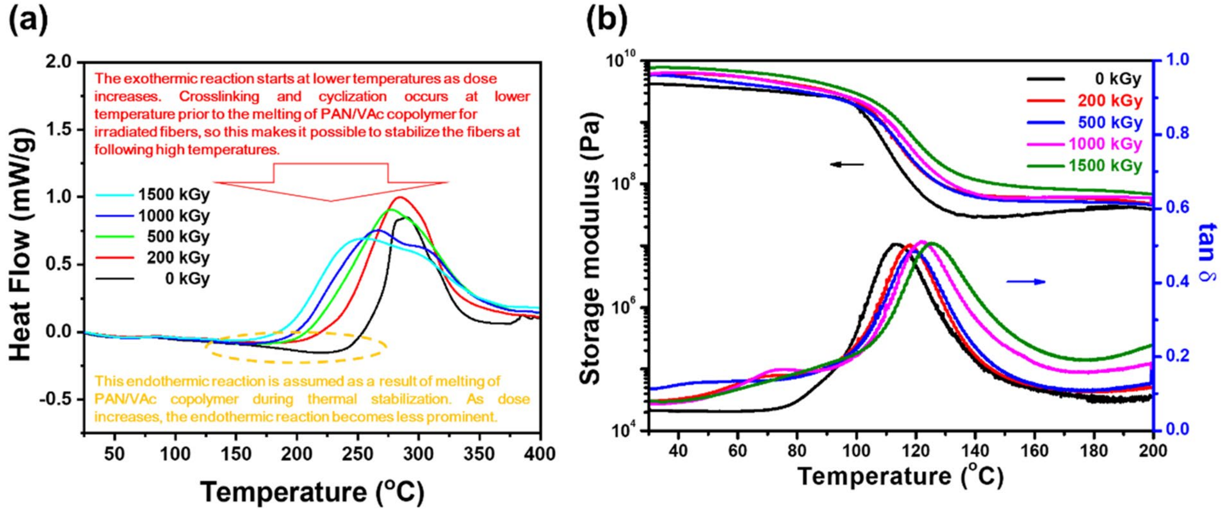

Fig. 9 **a** DSC and **b** DMA curves under dynamic stress of irradiated textile-grade PAN fibers at different doses. Reproduced and reprinted from [46], Copyright 2017, with permission from Elsevier

Fig. 10 **a**, **b** TS, **c**, **d** YM, and **e**, **f** STF of CFs fabricated based on different e-beam irradiation and subsequent thermal stabilization conditions. **a**, **c**, **e** Different doses and subsequent thermal stabilization under P1 condition. **b**, **d**, **f** Dose at 1000 kGy and different subsequent thermal stabilization conditions. Reprinted from [46], Copyright 2017, with permission from Elsevier

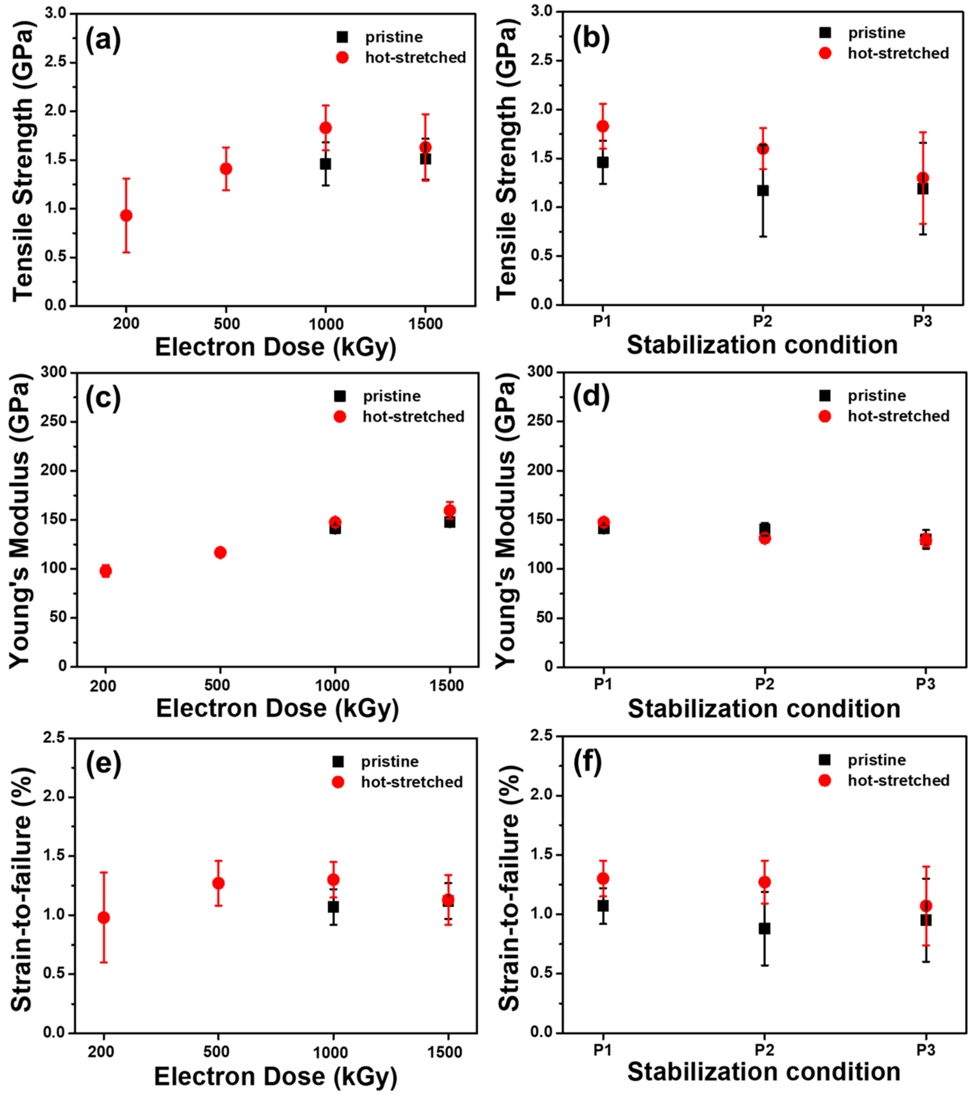

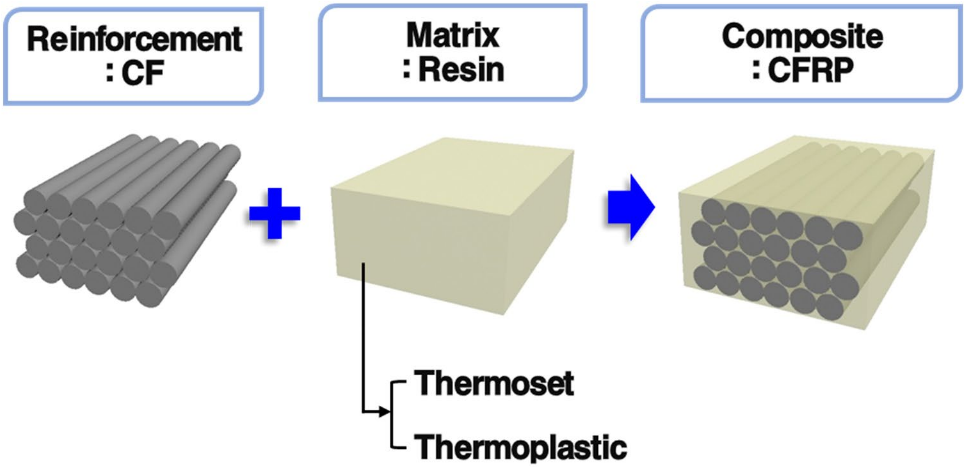

Fig. 11 Illustration of CFRP. CFs used as reinforcement surrounded in the polymer matrix. Thermoset or thermoplastic resin can be used as matrix material

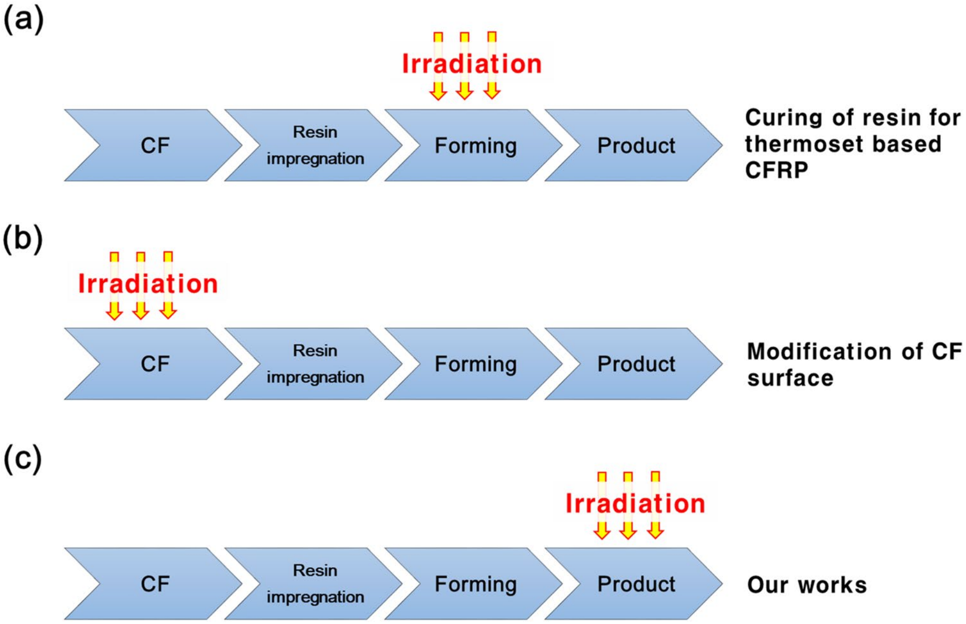

Fig. 12 Strategies to utilize e-beam irradiation for CFRPs. **a** In thermoset-resin-based CFRPs, curing via irradiation was investigated. **b** Surface modification of CFs via irradiation was investigated to improve interfacial properties of CF and resin. **c** CFRTPs were irradiated as post-treatment to improve their mechanical properties in our studies

surface and the dangling bond of the polymer. Several investigations are reported to improve the properties of CFRTPs via irradiation [66–68].

In our study, two typical thermoplastics, polyethylene (PE) and polypropylene (PP), were investigated as matrices of CFRTPs for high-energy e-beam irradiation. The dominant response upon irradiation differed significantly between PE (cross-linking) and PP (scission); therefore, the properties of CFRTPs are expected to be affected. First, the TS improved when the absorbed dose for high-density PE (HDPE)-based CFRTPs increased [69] (Fig. 13).

To determine the origin of this improvement, tensile testing and various measurements were performed on each component of the CFRTP (CF and HPDE). It was observed that the TS change of the CF was insignificant, whereas that of the HDPE increased slightly as the absorbed dose increased gradually. The major role of the matrix was load transfer to the CFs; therefore, the slight increase in the TS of the HDPE might be beneficial yet insufficient to explain the TS increment of the irradiated CFRTPs. As verified via spectroscopic analysis, various oxygen-containing functional groups were formed on the CFs and HDPE by irradiation, and we believe that strong attractive interactions occurred among these functional groups at the interface of the CFs and HDPE, which contributed significantly to the TS increase in the irradiated CFRTPs. The increased interfacial shear stress (IFSS) between the irradiated CFs and HDPE was confirmed via a fiber full-out test (Fig. 14). Furthermore, the irradiation-induced cross-linking of HDPE significantly enhanced the thermal stability of the CFRTPs. As shown in Fig. 15, the gel content reached ~ 90%, and the heat distortion temperature exceeded 300 °C for absorbed doses above 1200 kGy.

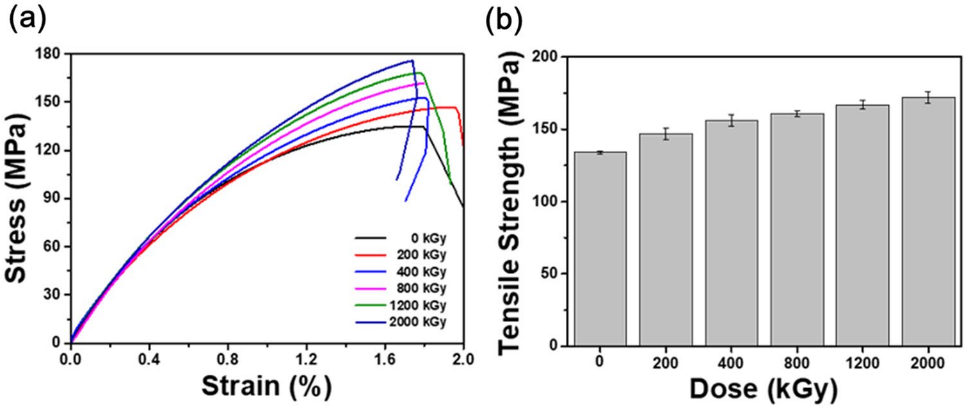

Fig. 13 **a** Stress–strain curve and **b** TS of HDPE-based CFRTPs irradiated for various absorbed doses. Reprinted from [69], Copyright 2020, with permission from Springer

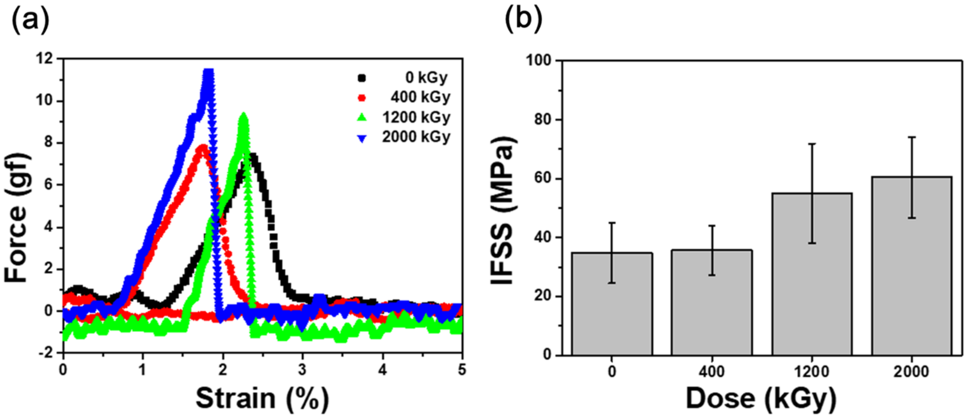

Fig. 14 **a** Force–strain curve and **b** IFSS for single CF–HDPE resin pull-out test for various absorbed doses. Reprinted from [69], Copyright 2020, with permission from Springer

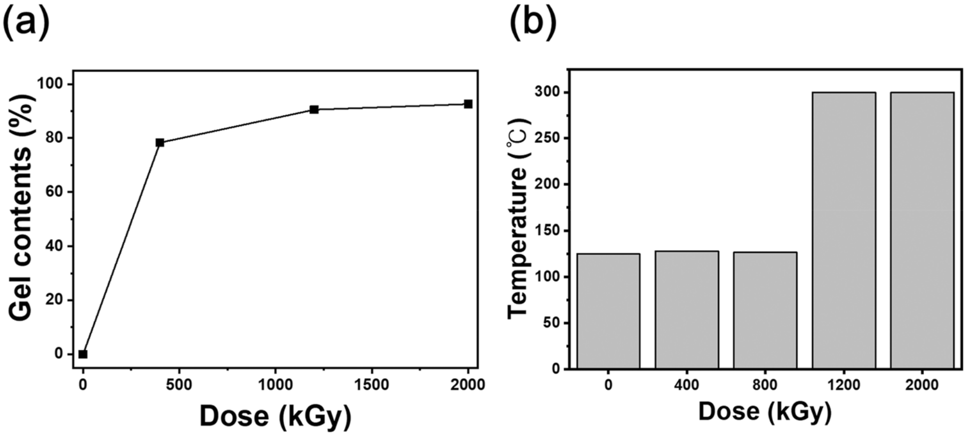

Fig. 15 **a** Gel contents and **b** heat distortion temperature of HDPE-based CFRTP for various absorbed doses. Reproduced from [69], Copyright 2020, with permission from Springer

Finally, it was concluded that e-beam irradiation exhibited two main effects: the cross-linking of the HDPE matrix facilitated the load transfer from the resin to the CF, and the formation of polar functional groups on the surface of the CF and HDPE provided attractive interactions at the interface between the CF and matrix (Fig. 16).

The effect of the absorbed dose rate on the TS and YM of the HDPE-based CFRTPs was further investigated at a fixed absorbed dose of 400 kGy (Fig. 17). Despite the same absorbed dose, the chemical composition differed depending on the absorbed dose rates, as shown in Table 4. By increasing the absorbed dose rates, the irradiation duration decreased, resulting in lower oxygen contents of the irradiated CFRTPs. Meanwhile, the TS of the CFs increased at higher absorbed dose rates. Consequently, these beneficial and detrimental effects maximized the TS of the irradiated CFRTPs at a certain absorbed dose rate (6.8 kGy/s) [70] (Fig. 18).

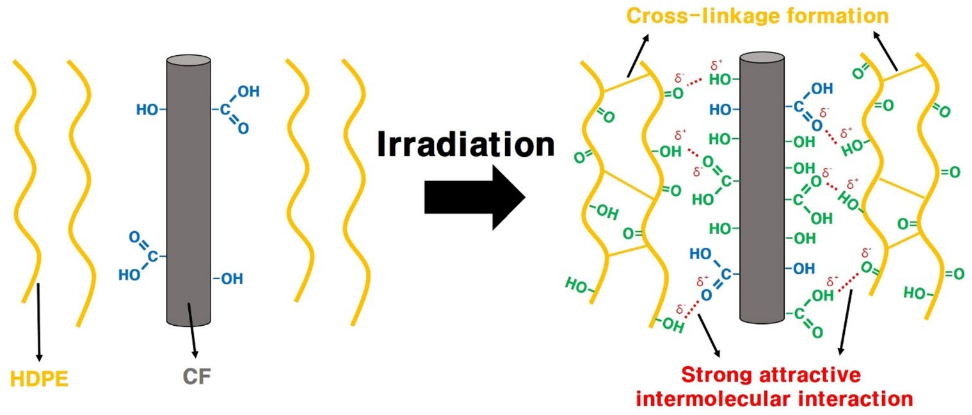

Fig. 16 Speculated intermolecular interaction between CF and HDPE of irradiated CFRTPs. Green characters represent functional groups formed by irradiation. Reprinted from [69], Copyright 2020, with permission from Springer

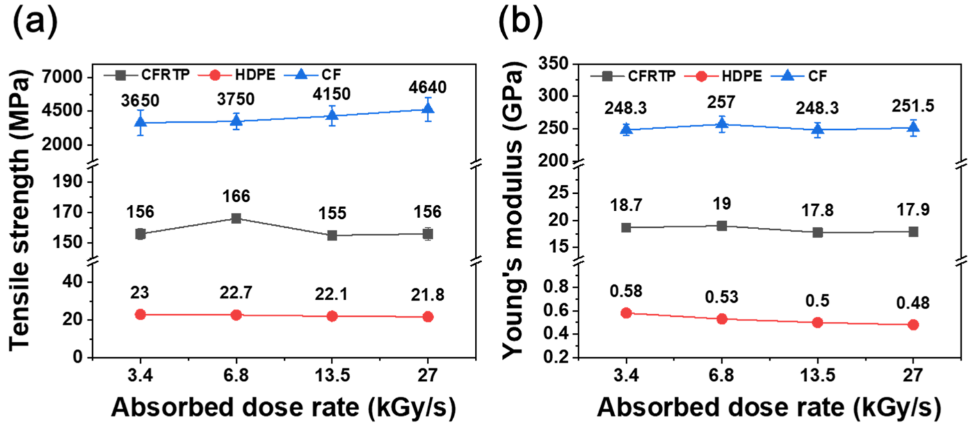

Fig. 17 **a** TS and **b** YM of CFRTP, HDPE, and CF irradiated at various absorbed dose rates. Reprinted from [70], Copyright 2020, with permission from MDPI

Table 4 Atomic percentage and C/O ratio of CFRTP, HDPE, and CF irradiated at various absorbed dose rates. Reprinted from [70], Copyright 2020, with permission from MDPI

	Absorbed dose rate (kGy/s)	At%					
		C1s	O1s	Na1s	N1s	Si2p	C/O ratio
CFRTP	3.4	89.3	7.25	1.23	1.12	1.09	12.31
	6.8	93.33	4.18	1.02	0.71	0.76	22.34
	13.5	94.38	3.83	0.68	0.63	0.47	24.62
	27	96.41	3.21	0.02	0.17	0.19	30.04
HDPE	3.4	84.51	10.28	1.7	2.2	1.3	8.22
	6.8	83.35	11.91	1.34	2.03	1.38	7
	13.5	91.22	5.77	0.66	1.52	0.82	15.82
	27	92.74	6.48	0	0.77	0	14.3
CF	3.4	78.51	16.92	–	2.01	2.56	4.64
	6.8	80.48	17.29	–	–	2.23	4.66
	13.5	80.1	15.09	–	2.31	2.5	5.31
	27	80.51	16.31	–	1.35	1.83	4.94

For the PP-based CFRTPs, changes in the TS and YM for various absorbed doses are shown in Fig. 19 [71]. Without the addition of a radiation cross-linker, the mechanical properties improved at low absorbed doses, whereas they deteriorated as the absorbed dose was further increased. As mentioned earlier, PP is a typical polymer that undergoes scission by irradiation; therefore, the efficient load transfer from PP to CFs was disrupted in the irradiated PP-based CFRTPs at high absorbed doses. The increase in the TS and YM at relatively low absorbed doses were attributed to the enhanced adhesion between PP and CF, similar to the case for the HDPE-based CFRTPs (Fig. 20). Therefore,

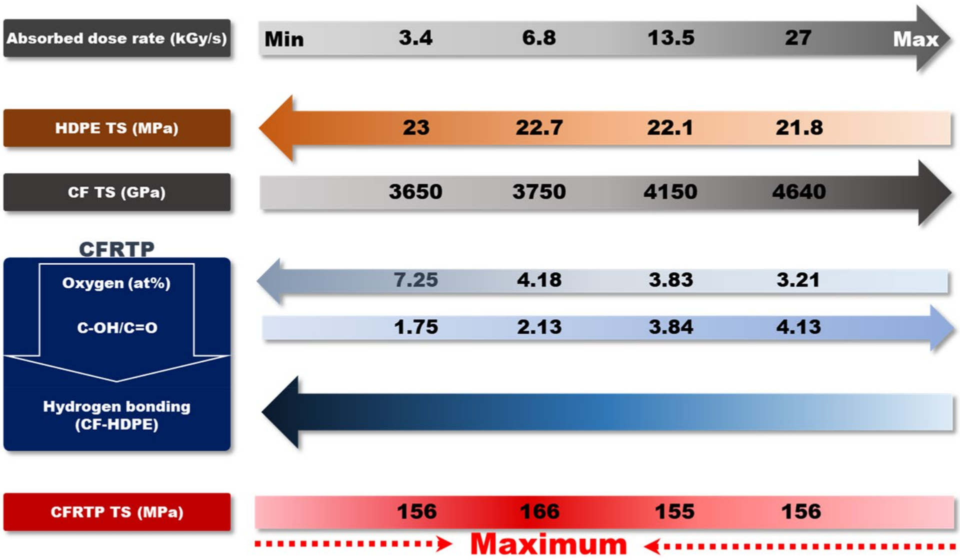

Fig. 18 Relationships of CFRTP TS vs. HDPE TS, CF TS, and CF–HDPE hydrogen bonding as a function of absorbed dose rates. Reprinted from [70], Copyright 2020, with permission from MDPI

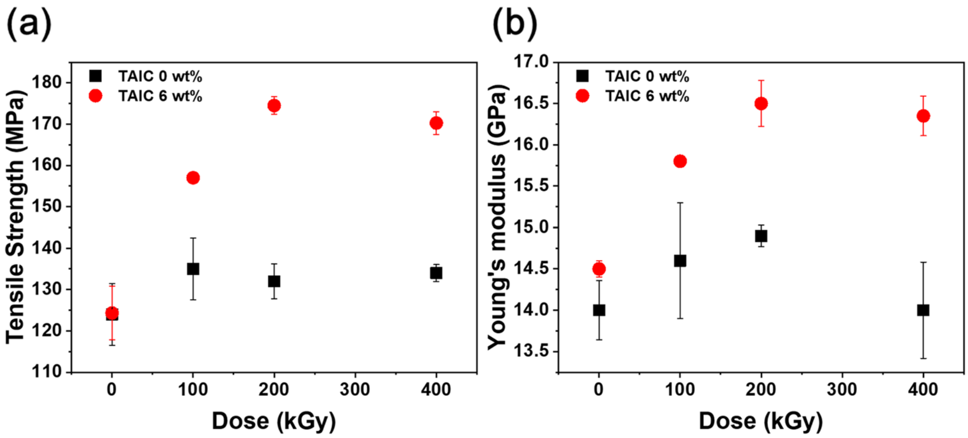

Fig. 19 **a** TS and **b** YM of PP-based CFRTPs irradiated for various absorbed doses. TAIC was added as radiation cross-linker. Reprinted from [71], Copyright 2020, with permission from Elsevier

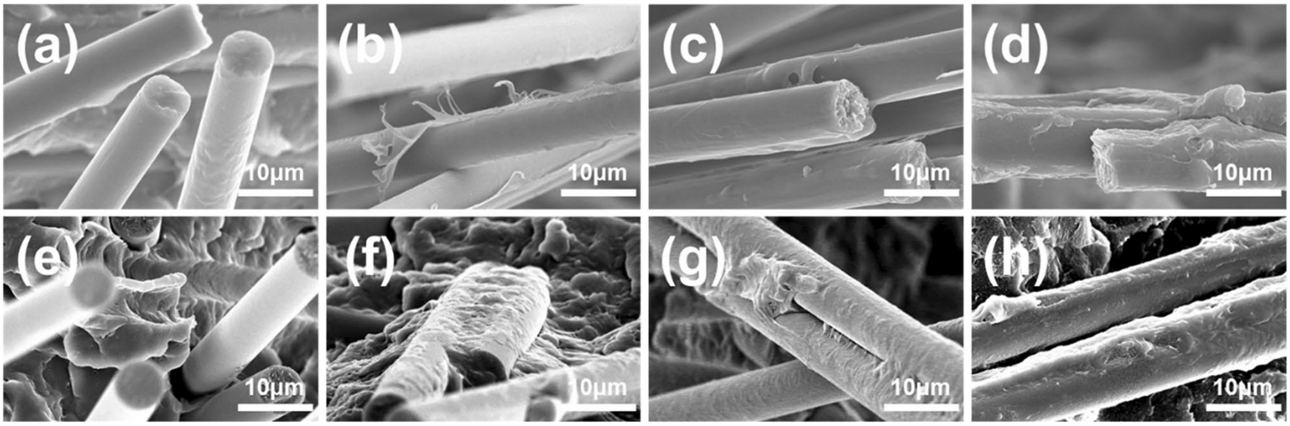

Fig. 20 SEM images of fracture surface of (a–d) CFRTP_0 wt% TAIC and (e–h) CFRTP_6 wt% TAIC dog-bone specimens after e-beam irradiation. Absorbed doses were **a**, **e** 0, **b**, **f** 100, **c**, **g** 200, and **d**, **h** 400 kGy. Reprinted from [71], Copyright 2020, with permission from Elsevier

Table 5 Evaluated data from TGA and DTG curves of CFRTP_0 wt% TAIC and CFRTP_6 wt% TAIC irradiated at various absorbed doses. Reprinted from [71], Copyright 2020, with permission from Elsevier

Dose (kGy)	CFRTP_0 wt% TAIC		CFRTP_6 wt% TAIC	
	T_{d5} (°C)	$T_{\text{-dM/dT,max}}$ (°C)	T_{d5} (°C)	$T_{\text{-dM/dT,max}}$ (°C)
0	369	424	364	470
100	380	447	385	451
200	399	466	401	474
400	398	460	403	490

a radiation cross-linker (triallyl isocyanurate, TAIC) was added to further enhance the mechanical properties of the irradiated PP-based CFRTPs. By optimizing the amount of TAIC added (6 wt%), the TS and YM increased significantly, as shown in Fig. 19. The introduction of TAIC contributed to the cross-linking of PP and the bonding between the CF and PP in the irradiated PP-based CFRTPs. Furthermore, the thermal properties were evaluated via thermogravimetric (TG) and derivative TG (DTG) analysis, which indicated the enhanced thermal stability of the irradiated PP-based CFRTPs containing TAIC (Table 5). Hence, we conclude that the mechanical and thermal properties of the PP-based CFRTP-containing TAIC can be improved via two irradiation effects: the cross-linking of PP and enhancement in the fiber–matrix interaction.

5 Conclusion

In this short review, the general aspects of radiation processing were explained. Compared with γ- or X-rays, e-beam has great advantage owing to its higher energy transfer rate that renders shorter irradiation duration. The key parameters of e-beam irradiation (energy, current, conveyor speed) and their relationship with penetration depth, absorbed dose, and dose rate were explained. Meanwhile, our studies related to the utilization of e-beam irradiation for preparing carbon fibers and improving properties of carbon-fiber-reinforced thermoplastics were reviewed. Based on our studies, e-beam irradiation was applied to fabricate low-cost CFs by shortening the conventional thermal stabilization process and using textile-grade PAN fibers as precursor. Furthermore, the mechanical and thermal properties of CFRTPs were improved via e-beam irradiation. Efficient load transfer from cross-linked thermoplastic matrix to CFs and the interfacial adhesion between CF and matrix were improved by irradiating CFRTPs. The thermal properties CFRTPs were enhanced by cross-linking the matrix via irradiation which overcame the intrinsic drawback of thermoplastics in high-temperature applications. As a result, we believe e-beam irradiation as a powerful, energy and cost-efficient tool to fabricate and improve carbon based advanced materials.

Acknowledgements This study was supported by a National Research Foundation of Korea (NRF) grant funded by the Korea government (MSIT) (Project Number: NRF-2021R1G1A1091519).

Declarations

Conflict of interests All authors declare no conflict of interests.

References

1. Morgan P (2005) Carbon fibers and their composites. CRC Press, Boca Raton
2. Lewandowska AE, Soutis C, Savage L, Eichhorn SJ (2015) Carbon fibres with ordered graphitic-like aggregate structures from a regenerated cellulose fibre precursor. Compos Sci Technol 116:50–57
3. Wang S, Li Y, Xiang H, Zhou Z, Chang T, Zhu M (2015) Low cost carbon fibers from bio-renewable lignin/poly (lactic acid)(PLA) blends. Compos Sci Technol 119:20–25
4. Maradur SP, Kim CH, Kim SY, Kim BH, Kim WC, Yang KS (2012) Preparation of carbon fibers from a lignin copolymer with polyacrylonitrile. Synth Met 162:453–459
5. Baker DA, Rials TG (2013) Recent advances in low-cost carbon fiber manufacture from lignin. J Appl Polym Sci 130:713–728
6. Jin FL, Lee SY, Park SJ (2013) Polymer matrices for carbon fiber-reinforced polymer composites. Carbon Lett 14:76–88
7. Sorina T, Gunyaev G (1995) Structural carbon-fibre-reinforced plastics and their properties. Polymer Matrix Compos 132–198
8. Jin FL, Park SJ (2015) Preparation and characterization of carbon fiber-reinforced thermosetting composites: a review. Carbon Lett 16:67–77
9. Nishida H, Carvelli V, Fujii T, Okubo K (2018) Thermoplastic vs. thermoset epoxy carbon textile composites. IOP Conf Ser Mater Sci Eng 406:012043
10. Yao SS, Jin FL, Rhee KY, Hui D, Park SJ (2018) Recent advances in carbon-fiber-reinforced thermoplastic composites: a review. Compos B Eng 142:241–250
11. Cleland MR, Parks LA, Cheng S (2003) Applications for radiation processing of materials. Nucl Instrum Methods Phys Res B 208:66–73
12. Chmielewski AG, Haji-Saeid M, Ahmed S (2005) Progress in radiation processing of polymers. Nucl Instrum Methods Phys Res B 236:44–54
13. Clough RL (2001) High-energy radiation and polymers: a review of commercial processes and emerging applications. Nucl Instrum Methods Phys Res B 185:8–33
14. Kempner ES (2011) Direct effects of ionizing radiation on macromolecules. J Polym Sci B Polym Phys 49:827–831
15. Kil HS, Lee S (2019) High flame retardancy of oxidized polyacrylonitrile fibers prepared by effective plasma-assisted thermal stabilization and electron-beam irradiation. Composites B Eng 178:107458
16. Saif MJ, Naveed M, Asif HM, Akhtar R (2018) Irradiation applications for polymer nano-composites: a state-of-the-art review. J Ind Eng Chem 60:218–236
17. Chmielewski AG, Haji-Saeid M (2004) Radiation technologies: past, present and future. Radiat Phys Chem 71:17–21
18. Ashfaq A, Clochard MC, Coqueret X, Dispenza C, Driscoll MS, Ulański P, Al-Sheikhly M (2020) Polymerization reactions

and modifications of polymers by ionizing radiation. Polymers 12:2877

19. Ferry M, Ngono Y (2020) Energy transfer in polymers submitted to ionizing radiation: a review. Radiat Phys Chem 180:109320
20. Burgstaller C, Höftberger T, Gallnböck-Wagner B, Stadlbauer W (2021) Effects of radiation type and dose on the properties of selected polymers. Polym Eng Sci 61:39–54
21. Kudoh H, Celina M, Malone GM, Kaye RJ, Gillen KT, Clough RL (1996) Pulsed e-beam irradiation of polymers—a comparison of dose rate effects and let effects. Radiat Phys Chem 48:555–562
22. Soulis S, Konstantopoulos G, Koumoulos EP, Charitidis CA (2020) Impact of alternative stabilization strategies for the production of PAN-based carbon fibers with high performance. Fibers 8:33
23. Saha B, Schatz GC (2012) Carbonization in polyacrylonitrile (PAN) based carbon fibers studied by ReaxFF molecular dynamics simulations. J Phys Chem B 116:4684–4692
24. Rahaman MSA, Ismail AF, Mustafa A (2007) A review of heat treatment on polyacrylonitrile fiber. Polym Degrad Stab 92:1421–1432
25. Dietrich J, Hirt P, Herlinger H (1996) Electron-beam-induced cyclisation to obtain C-fibre precursors from polyacrylonitrile homopolymers. Eur Polym J 32:617–623
26. Shin HK, Park M, Kim HY, Park SJ (2015) An overview of new oxidation methods for polyacrylonitrile-based carbon fibers. Carbon Lett 16:11–18
27. Yuan H, Wang Y, Liu P, Yu H, Ge B, Mei Y (2011) Effect of electron beam irradiation on polyacrylonitrile precursor fibers and stabilization process. J Appl Polym Sci 122:90–96
28. Park M, Choi Y, Lee SY, Kim HY, Park SJ (2014) Influence of electron-beam irradiation on thermal stabilization process of polyacrylonitrile fibers. J Ind Eng Chem 20:1875–1878
29. Shin HK, Jeun JP, Kang PH (2012) The characterization of polyacrylonitrile fibers stabilized by electron beam irradiation. Fibers Polym 13:724–728
30. Shin HK, Park M, Kim HY, Park SJ (2015) Influence of oxidative atmosphere of the electron beam irradiation on cyclization of PAN-based fibers. Carbon Lett 16:219–221
31. Zhang W, Wang M, Zhang W, Liu W, Yang C, Shen R, Wu G (2018) Significantly reduced pre-oxidation period of PAN fibers by continuous electron beam irradiation: optimization by monitoring radical variation. Polym Degrad Stab 158:72–82
32. Zhang W, Wang M, Liu W, Yang C, Wu G (2019) Higher dose rate effect of 500-keV EB irradiation favoring free radical annealing and pre-oxidation of polyacrylonitrile fibers. Polym Degrad Stab 167:201–209
33. Tarakanov BM (1996) Effect of γ-radiation on the structure and thermal properties of polyacrylonitrile fibres. Fibre Chem 27:150–154
34. Zhou L, Lu Y, Zhao W, Yang C, Jiang J (2016) Effects of gamma ray irradiation on poly (acrylonitrile-co-methyl acrylate) fibers. Polym Degrad Stab 128:149–157
35. Liu W, Wang M, Xing Z, Qi Y, Wu G (2012) Radiation-induced crosslinking of polyacrylonitrile fibers and the subsequent regulative effect on the preoxidation process. Radiat Phys Chem 81:622–627
36. Tan L, Wan A (2011) Structural changes of polyacrylonitrile precursor fiber induced by γ-ray irradiation. Mater Lett 65:3109–3111
37. Zhao W, Lu Y, Jiang J, Hu L, Zhou L (2015) The effect of γ-ray irradiation on the microstructure and thermal properties of polyacrylonitrile fibers. RSC Adv 5:23508–23518
38. Liu W, Wang M, Xing Z, Wu G (2014) Radiation oxidation and subsequent thermal curing of polyacrylonitrile fiber. Radiat Phys Chem 94:9–13
39. Liu S, Liu R, Han K, Liu H, Yu M (2016) Influence of γ-ray irradiation on structure and properties of PAN precursor fibers. Polym Eng Sci 56:1313–1318
40. Park S, Yoo SH, Kang HR, Jo SM, Joh HI, Lee S (2016) Comprehensive stabilization mechanism of electron-beam irradiated polyacrylonitrile fibers to shorten the conventional thermal treatment. Sci Rep 6:1–9
41. Choi D, Kil HS, Lee S (2019) Fabrication of low-cost carbon fibers using economical precursors and advanced processing technologies. Carbon 142:610–649
42. Liu Y, Huang X, Liu J, Liang J, Wang X (2020) Structure and tensile properties of carbon fibers based on electron-beam irradiated polyacrylonitrile fibers. J Mater Sci 55:4962–4969
43. Yang J, Liu Y, Liu J, Shen Z, Liang J, Wang X (2018) Rapid and continuous preparation of polyacrylonitrile-based carbon fibers with electron-beam irradiation pretreatment. Materials 11:1270
44. Zhao W, Lu Y, Zhou L, Jiang J, Wang J, Chen Q, Tian F (2016) Effects on the oriented structure and mechanical properties of carbon fibers by pre-irradiating polyacrylonitrile fibers with γ ray. J Mater Sci 51:7073–7084
45. Zhao W, Lu Y, Wang J, Chen Q, Zhou L, Jiang J, Chen L (2016) Improving crosslinking of stabilized polyacrylonitrile fibers and mechanical properties of carbon fibers by irradiating with γ-ray. Polym Degrad Stab 133:16–26
46. Yoo SH, Park S, Park Y, Lee D, Joh HI, Shin I, Lee S (2017) Facile method to fabricate carbon fibers from textile-grade polyacrylonitrile fibers based on electron-beam irradiation and its effect on the subsequent thermal stabilization process. Carbon 118:106–113
47. Jin X, Feng C, Creighton C, Hameed N, Parameswaranpillai J, Salim NV (2021) On the structural evolution of textile grade polyacrylonitrile fibers during stabilization and carbonization: towards the manufacture of low-cost carbon fiber. Polymer Degrad Stab 186:109536
48. Sedghi A, Farsani RE, Shokuhfar A (2008) The effect of commercial polyacrylonitrile fibers characterizations on the produced carbon fibers properties. J Mater Process Technol 198:60–67
49. Friedrich K, Almajid AA (2013) Manufacturing aspects of advanced polymer composites for automotive applications. Appl Compos Mater 20:107–128
50. Zhao X, Duan Y, Li D, Wang B, Zhang X (2015) Investigation of curing characteristics of carbon fiber/epoxy composites cured with low-energy electron beam. Polym Compos 36:1731–1737
51. Glauser T, Johansson M, Hult A (1999) Electron-beam curing of thick thermoset composite matrices. Polymer 40:5297–5302
52. Vautard F, Fioux P, Vidal L, Siffer F, Roucoules V, Schultz J, Nardin M, Defoort B (2014) Use of plasma polymerization to improve adhesion strength in carbon fiber composites cured by electron beam. ACS Appl Mater Interfaces 6:1662–1674
53. Berejka AJ, Eberle C (2002) Electron beam curing of composites in North America. Radiat Phys Chem 63:551–556
54. Kim BH, Lee DH, Yang KS, Lee BC, Kim YA, Endo M (2011) Electron beam irradiation-enhanced wettability of carbon fibers. ACS Appl Mater Interfaces 3:119–123
55. Zhenjuan Z, Yuansheng W, Qinyi D, Siliang W, Te H (2013) Surface modification of carbon fiber via electron-beam irradiation grafting. Surf Interface Anal 45:913–918
56. Tiwari S, Bijwe J (2014) Surface treatment of carbon fibers-a review. Proc Technol 14:505–512
57. Mahieux CA (2001) Cost effective manufacturing process of thermoplastic matrix composites for the traditional industry: the example of a carbon-fiber reinforced thermoplastic flywheel. Compos Struct 52:517–521
58. Sudhin AU, Remanan M, Ajeesh G, Jayanarayanan K (2020) Comparison of properties of carbon fiber reinforced thermoplastic and thermosetting composites for aerospace applications. Mater Today Proc 24:453–462

59. Alshammari BA, Alsuhybani MS, Almushaikeh AM, Alotaibi BM, Alenad AM, Alqahtani NB, Alharbi AG (2021) Comprehensive review of the properties and modifications of carbon fiber-reinforced thermoplastic composites. Polymers 13:2474
60. Tsuchikura N, Faudree MC, Nishi Y (2013) Charpy impact value of sandwich structural (CFRP/ABS/CFRP) composites constructed with carbon fiber reinforced epoxy polymer (CFRP) and acrylonitrile butadiene styrene (ABS) sheets separately irradiated by electron beam prior to lamination. Mater Trans 54:371–379
61. Takei H, Salvia M, Vautrin A, Tonegawa A, Nishi Y (2011) Effects of electron beam irradiation on elasticity of CFRTP (CF/PEEK). Mater Trans 52:734–739
62. Nishi Y, Takei H, Iwata K, Salvia M, Vautrin A (2009) Effects of electron beam irradiation on impact value of carbon fiber reinforced thermoplastic polyetheretherketone. Mater Trans 50:2826–2832
63. Takei H, Iwata K, Salvia M, Vautrin A, Nishi Y (2010) Effects of electron beam irradiation on impact value of novolak-type phenol CFRTP. Mater Trans 51:2259–2265
64. Nishi Y, Mizutani A, Uchida N (2004) Electron beam strengthening for carbon fiber-reinforced composite materials. J Thermoplast Compos Mater 17:289–302
65. Sasuga T, Seguchi T, Sakai H, Nakakura T, Masutani M (1989) Electron-beam irradiation effects on mechanical properties of PEEK/CF composite. J Mater Sci 24:1570–1574
66. Szabó L, Imanishi S, Tetsuo F, Nishio M, Hirose D, Tsukegi T, Taki K, Ninomiya K, Takahashi K (2019) Electron beam induced strengthening of a short carbon fiber reinforced green thermoplastic composite: key factors determining materials performance. Compos A Appl Sci Manuf 121:386–396
67. Karsli NG, Aytac A, Akbulut M, Deniz V, Güven O (2013) Effects of irradiated polypropylene compatibilizer on the properties of short carbon fiber reinforced polypropylene composites. Radiat Phys Chem 84:74–78
68. Hassan MM, El-Hag Ali A, Mahoud GA, Hegazy ESA (2005) Synergistic effect of short reinforced fibers and gamma rays on the thermal and mechanical properties of waste poly (propylene) composites. J Appl Polym Sci 96:1741–1747
69. Jung S, Park SK, Ghim HD, Lee DY, Yoo SH (2020) Synergetic effect of cross-linking and interfacial interaction in carbon fiber reinforced thermoplastic to enhance its tensile strength by electron-beam irradiation. Carbon Lett 30:165–175
70. Park SK, Choi DY, Choi DY, Lee DY, Yoo SH (2020) Influences of absorbed dose rate on the mechanical properties and fiber-matrix interaction of high-density polyethylene-based carbon fiber reinforced thermoplastic irradiated by electron-beam. Polymers 12:3012
71. Park SK, Jung S, Lee DY, Ghim H, Yoo SH (2020) Effects of electron-beam irradiation and radiation cross-linker on tensile properties and thermal stability of polypropylene-based carbon fiber reinforced thermoplastic. Polymer Degrad Stab 181:109301